Dependence of the Superconducting Transition Temperature on the Doping Level in Single-Crystalline Diamond Films

E. Bustarret,[1] J. Kačmarčik,[2,3] C. Marcenat,[2] E. Gheeraert,[1] C. Cytermann,[4] J. Marcus,[1] and T. Klein[1,5]

[1]*Laboratoire d'Etudes des Propriétés Electroniques des Solides, CNRS, B.P.166, 38042 Grenoble Cedex 9, France*

[2]*Commissariat à l'Energie Atomique - Grenoble, Département de Recherche Fondamentale sur la Matière Condensée, SPSMS, 17 rue des Martyrs, 38054 Grenoble Cedex 9, France*

[3]*Centre of Low Temperature Physics IEP Slovakian Academy of Sciences & FS UPJŠ, Watsonova 47, 043 53 Košice, Slovakia*

[4]*Solid State Institute, Technion, 32000 Haifa, Israel*

[5]*Institut Universitaire de France and Université Joseph Fourier, B.P.53, 38041 Grenoble Cedex 9, France*

(Received 5 August 2004; published 1 December 2004)

Homoepitaxial diamond layers doped with boron in the 10^{20}–10^{21} cm^{-3} range are shown to be type II superconductors with sharp transitions (~ 0.2 K) at temperatures increasing from 0 to 2.1 K with boron contents. The critical concentration for the onset of superconductivity in those 001-oriented single-crystalline films is about 5–7 10^{20} cm^{-3}. The $H - T$ phase diagram has been obtained from transport and ac-susceptibility measurements down to 300 mK.

DOI: 10.1103/PhysRevLett.93.237005 PACS numbers: 74.25.Op, 73.61.Cw

Type II superconductivity has been recently reported for heavily boron-doped polycrystalline diamond prepared either as bulk [1] or thin film samples [2], providing a new interesting system for the study of superconductivity in doped semiconductors. Based on the great bonding strength of the valence band states and on their strong coupling to the carbon lattice phonons, various theoretical studies [3,4] have stressed the similarity between diamond and the recently discovered MgB_2 system which shows a surprisingly high T_c value on the order of 40 K. Those calculations lead to T_c values in the 0.2 to 25 K range (depending on the boron content), but ignore the boron impurity band [3,4]. An alternative theoretical approach [5] stresses out the fact that the boron concentration range where superconductivity has been observed is close to the Anderson-Mott metal-insulator transition and suggests an electron correlation driven extended *s*-wave superconductivity in the boron impurity band.

In order to bring new quantitative constraints on the theoretical models proposed for superconductivity in diamond, we undertook an experimental investigation of the dependence of the superconducting transition temperature on the doping boron concentration. In this Letter, we report on magnetic and transport experiments on a set of high quality single-crystalline epilayers doped in the relevant 10^{20}–10^{21} cm^{-3} range. We show that T_c rapidly increases above some critical concentration $\sim$5–7 $\times$ 10^{20} cm^{-3} reaching $\sim$2 K for $n_B = 19 \times 10^{20}$ cm^{-3} (see Table I).

001-oriented type Ib diamond substrates were first exposed to a pure hydrogen plasma. Methane (4%) was subsequently introduced and a 0.5 μm-thick buffer layer of nonintentionally doped material was deposited at 820°C by the microwave plasma-assisted decomposition (MPCVD) of the gas mixture at a total pressure of 30 Torr. Finally, diborane was introduced in the vertical silica wall reactor with boron to carbon concentration ratios in the gas phase [$(B/C)_{gas}$] ranging from 1500 to 3000 ppm. With a typical growth rate of 0.9 μm/h these deposition conditions led to 0.1 to 4 μm-thick p^+-type diamond layers. Secondary ion mass spectroscopy (SIMS) depth profiles of $^{11}B^-$, $^{12}C^-$ and $^{11}B^{12}C^-$ ions (masses $m = 11$, 10, and 23, respectively) were measured using a Cs^+ primary ion beam in a Cameca Ims $4f$ apparatus. As shown in Fig. 1 for samples 2, 4, and 5, these profiles were found to be flat or with a slow decrease toward the buffer layer. The boron atomic densities n_B shown both in Fig. 1 and Table I were derived from a quantitative comparison to a SIMS profile measured under the same conditions in a B-implanted diamond crystal with a known peak boron concentration of 2.4×10^{20} cm^{-3}. For thin enough samples, the profile yielded also the residual doping level in the buffer layer, around 10^{18} cm^{-3}. Moreover, the single crystal and epitaxial character of the MPCVD layers was checked by high resolution x-ray diffraction, yielding shifted narrow lines with smaller linewidths at half maximum than for the Ib substrate (typically 10 arc sec for the 004 Bragg peak of the epilayer, instead of 13 arc sec for the substrate). The chemical composition [6], structural [7,8], and optical

TABLE I. Sample characteristics—thickness (t), gas phase ratio [$(B/C)_{gas}$], boron concentration (n_B), and critical temperature (T_c) for the studied diamond epitaxial films.

Sample	t(μm)	$(B/C)_{gas}$(ppm)	n_B(10^{20} cm^{-3})	T_c(K)
1	3.0	1615	3.6	≤ 0.05
2	3.0	1730	9	0.9
3	3.0	1845	10	1.2
4	2.0	2200	11.5	1.4
5	0.15	2800	19	2.1

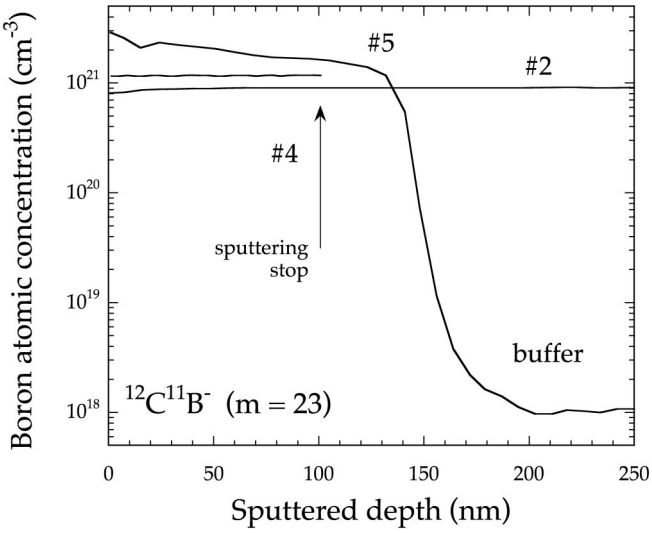

FIG. 1. SIMS profiles for ion mass $m = 23$ obtained using Cs^+ primary ions on samples 2, 4, and 5. In the case of the thicker samples, sputtering was interrupted before reaching the buffer layer.

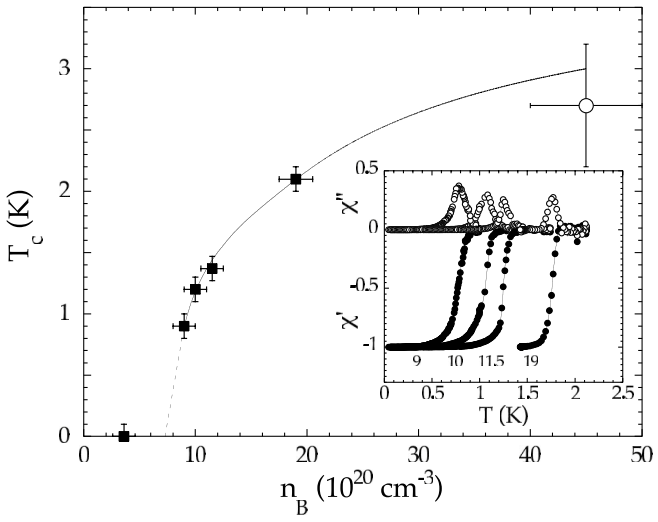

FIG. 2. Dependence of the superconducting transition temperature T_c on the boron concentration n_B: solid squares—this work, open circles—from [1]. The different T_c values were obtained from the onset of the diamagnetic signal (see inset for the real (solid symbols) and imaginary (open symbols) parts of the magnetic susceptibility.

[6,7,9] characteristics of these layers at room temperature are well documented and have been reviewed recently, together with some preliminary transport measurements [7].

The superconducting temperatures have been deduced from ac-susceptibility measurements (χ_{ac}). The films have been placed on top of miniature coils and T_c has been obtained by detecting the change in the self induction of the coils induced by the superconducting transitions. For fully screening samples, we observed a 4% drop of the induction $L(\sim 1$ mH). Small ac-excitation fields ($\omega \sim 99$ kHz and $h_{ac} \sim$ a few mG) have been applied perpendicularly to the films. Four Au/Ti electrodes were deposited on top of the film with the highest T_c for magneto-transport measurements. A very small current ($\sim 1nA$) corresponding to a current density on the order of 10^{-3} Acm^{-2} has been used to avoid flux flow dissipation. A standard lock-in technique at 17 Hz was used to measure the temperature dependencies of the sample resistance at fixed magnetic fields. The measurements were performed down to 50 mK (χ_{ac}) and 300 mK (transport) and the magnetic field was applied perpendicularly to the doped plane of the sample.

The critical temperatures (see Table I) reported in Fig. 2 have been deduced from the onset of the diamagnetic signal (see inset of Fig. 2). The susceptibility has been rescaled to -1 in the superconducting state and a $N \sim 0.9$ demagnetization coefficient has been used (the values of T_c do not depend on this choice). This choice for N leads to a dissipation peak on the order of 0.2–0.3 as expected for the non linear regime. This is consistent with the observation of a slight increase of the width of the transition for increasing h_{ac} values. As shown in the inset of Fig. 2 (and in Fig. 3), the transitions are very sharp (with a width $\sim$0.2 K) allowing an accurate determination of T_c and stressing out the high quality of our samples. For comparison, the polycrystalline samples measured in previous reports presented a much larger resistivity transition width, $\sim$1.7 K in [1] and $\sim$2.6 K in [2].

No transition was observed down to 50 mK for the film with $n_B = 3.6 \times 10^{20}$ cm^{-3}. For higher boron concentrations, T_c increases rapidly with doping above some critical concentration ~ 5–7×10^{20} cm^{-3} reaching 2.1 K for $n_B = 19 \times 10^{20}$ at. cm^{-3}. The dependence of T_c with doping extrapolates towards the data recently obtained by [1]. On the contrary, our T_c value for $n_B \sim 10^{21}$ cm^{-3} ($\sim$ 1 K) is much lower than the one recently reported by [2] ($\sim$ 4–7 K). The present data obtained on 001-oriented epilayers suggest that these authors have largely underestimated the boron concentration of their polycrystalline samples. They deduced this concentration from Hall measurements which are known to give results that deviate significantly from the actual boron concentration in p^+-type diamond [7]. It is also worth noticing that we observed superconducting transitions with T_c on the order of 1 K for boron contents $\sim$0.5 at. % whereas recent calculations of the electron-phonon coupling led to much smaller T_c values for these doping levels [3–5].

The influence of an external field on the superconducting transition is displayed in Fig. 3. As shown in panel a, the transition is shifted towards lower temperatures as the magnetic field is increased. The transition width remains relatively small up to $\sim$1 T and rapidly increases for larger fields. In the absence of thermodynamic measure-

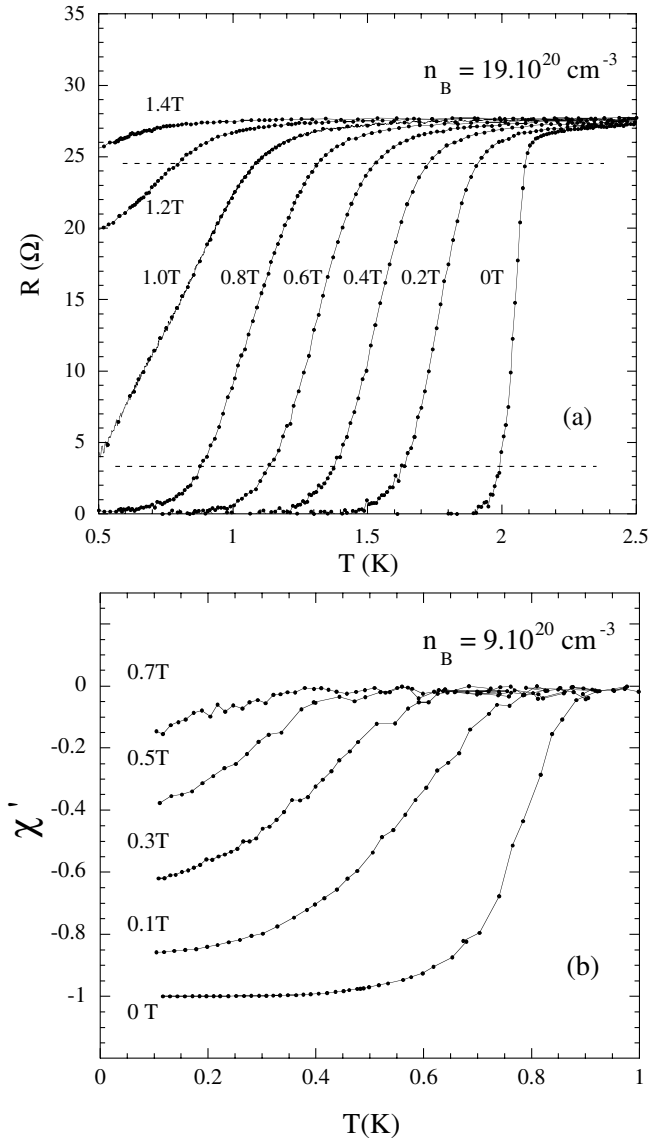

FIG. 3. (a) Temperature dependence of the electrical resistance at indicated magnetic fields for the film with $n_B = 19 \times 10^{20}$ at. cm^{-3}. The dashed lines correspond to the two criteria used for the determination of H_{c2} (see Fig. 4), i.e., $R/R_N =$ 90% and 10% (R_N being the normal state resistance). (b) Temperature dependence of the real part of the magnetic susceptibility at indicated magnetic fields for the film with $n_B = 9 \times 10^{20}$ at. cm^{-3}. H_{c2} has been deduced from the onset of the diamagnetic signal.

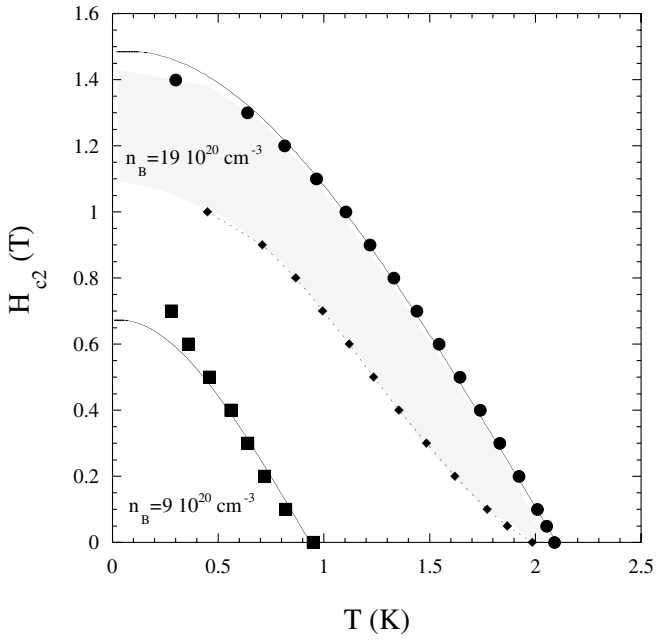

FIG. 4. $H - T$ phase diagram for the films with $n_B = 19 \times 10^{20}$ at. cm^{-3} and $n_B = 9 \times 10^{20}$ at. cm^{-3}. The solid circles (diamonds) have being deduced from temperature sweeps of the electrical resistance [see Fig. 3(a)] for $R/R_N = 90\%$ ($R/R_N = 10\%$). The gray area is an indication of the width of the transition. The solid squares were defined from the onset of the ac susceptibility [see Fig. 3(b)]. The solid lines are fits to the data using classical theory [10], for which the only free parameter is $H_{c2}(0)$. The dotted line is a guide to the eye.

ments, some care should be taken in order to define an accurate H_{c2} line. This line has been defined from the classical $R/R_N = 90\%$ criterion (where R_N is the normal state resistance corresponding to a resistivity $\rho_N \sim$ 0.5 mΩ cm for sample 5). As shown in Fig. 4, the corresponding $H_{c2}(T)$ line can be well described by classical theory [10]. We hence get $H_{c2}(0) \sim 1.4$ T corresponding to a coherence length $\xi_0 = \sqrt{\Phi_0/2\pi H_{c2}(0)} \sim 150$ Å for $n_B = 19 \times 10^{20}$ cm^{-3} (Φ_0 being the flux quantum). We have also reported in Fig. 4 the line corresponding to $R/R_N = 10\%$, which gives an indication for the width of the transition, pointing out that the transition curves rapidly increase for $H > 1$ T. Such a broadening may suggest the presence of quantum fluctuations as also indicated by the almost temperature-independent mixed state resistivity above 1.2 T. The strength of these fluctuations can be quantified through the quantity $Q_u = R_{\text{eff}}/R_Q$ where $R_Q = \hbar/e^2 \sim 4.1$ kΩ is the quantum resistance and $R_{\text{eff}} = \rho_N/s$ (s is a relevant length scale for these fluctuations [11]). Taking $\rho_N \sim 5 \times 10^{-4}$ Ω cm and $s \sim \xi(0) \sim 150$ Å for sample 5, we obtain a large Q_u ratio $\sim$0.1, being on the order of the Q_u values reported in other systems in which quantum fluctuations are present [12,13].

For sample 2, the H_{c2} line has been deduced from the shift of the diamagnetic response with increasing fields. In this case, the rapid broadening of the transition is the hallmark of a small critical current density (J_c) again emphasizing the high quality of our films. Indeed, in the nonlinear regime, the susceptibility is directly related to $J_c d/h_{\text{ac}}$ (where d is a characteristic length scale on the order of the sample thickness) and $J_c \approx h_{\text{ac}}/d \sim$ 1 Acm^{-2} for $\chi' \sim -0.4$. In this case, no saturation was observed down to 200 mK, indicating some deviation

from the classical behavior. Note that for both samples the slope $[dH_{c2}/dT]_{T\to 0} \sim 1$ T/K, is almost 2 times smaller than the value reported by Ekimov *et al.* [1].

On the basis of the criterion first proposed by Mott [14] for metal-nonmetal transitions, which in its final form ($N_c^{1/3} a_H = 0.26$, where a_H is the Bohr radius) has been verified in a wide variety of condensed media [15], the critical concentration in *p*-type diamond is expected to be around $N_c = 2 \times 10^{20}$ cm^{-3} [16]. The boron doping range where zero field superconductivity disappears (see Fig. 2), $5\text{–}7 \times 10^{20}$ cm^{-3}, is thus expected to lie on the metallic side of the metal-insulator transition (MIT) for this system. The accuracy of Mott's criterion, also tested recently for other wide band gap semiconductors [17], is limited by the discrepancies in the values proposed in the literature for the acceptor Bohr radius a_H, in line with other inconsistencies about the valence band parameters of diamond [18]. The experimental case for the MIT being still open for diamond [7,19,20], specific transport studies should be undertaken at low temperature on both 001 and 111-oriented single crystals. Measurements of the actual carrier concentration in the relevant doping range would establish whether the interesting situation where the proximity of the MIT affects the superconductive transition [21] also occurs in diamond.

To conclude, we were able to prepare highly homogeneous and well characterized boron-doped diamond films in the 10^{20}–10^{21} cm^{-3} range where superconductivity occurs. Sharp transitions (~ 0.2 K wide) were observed above a critical concentration on the order of $5\text{–}7 \times 10^{20}$ cm^{-3}. Quantum effects may play a significant role in this system as suggested by the large quantum resistance ratio $Q_u \sim 0.1$.

We are grateful to F. Pruvost who grew some of the diamond layers and to Dr. L. Ortega (Cristallographie, CNRS, Grenoble) for the x-ray diffraction experiments.

[1] E. A. Ekimov, V. A. Sidorov, E. D. Bauer, N. N. Melnik, N. J. Curro, J. D. Thompson, and S. M. Stishov, Nature (London) **428**, 542 (2004).
[2] Y. Takano, M. Nagao, K. Kobayashi, H. Umezawa, I. Sakaguchi, M. Tachiki, T. Hatano, and H. Kawarada, cond-mat/0406053.
[3] L. Boeri, J. Kortus, and O. K. Andersen, cond-mat/0404447.
[4] K.W. Lee and W. E. Pickett, cond-mat/0404286.
[5] G. Baskaran, cond-mat/0404286.
[6] E. Bustarret, F. Pruvost, M. Bernard, C. Cytermann, and C. Uzan-Saguy, Phys. Status Solidi A **186**, 303 (2001).
[7] E. Bustarret, E. Gheeraert, and K. Watanabe, Phys. Status Solidi A **199**, 9 (2003).
[8] F. Brunet, P. Germi, M. Pernet, A. Deneuville, E. Gheeraert, F. Laugier, M. Burdin, and G. Rolland, Diam. Relat. Mater. **7**, 869 (1998).
[9] F. Pruvost, E. Bustarret, and A. Deneuville, Diam. Relat. Mater. **9**, 295 (2000).
[10] L. P. Gor'kov, JETP Lett. **10**, 593 (1960).
[11] G. Blatter, B. Ivlev, Y. Kagan, M. Theunissen, Y. Volokitin, and P. Kes, Phys. Rev. B **50**, 13 013 (1994).
[12] A. Yazdani and A. Kapitulnik, Phys. Rev. Lett. **74**, 3037 (1995).
[13] S. Okuma, Y. Imamoto, and M. Morita, Phys. Rev. Lett. **86**, 3136 (2001).
[14] N. F. Mott, Can. J. Phys. **34**, 1356 (1956).
[15] P. P. Edwards and M. J. Sienko, Phys. Rev. B **17**, 2575 (1978).
[16] H. Shiomi, Y. Nishibayashi, and N. Fujimori, Jpn J. Appl. Phys. **30**, 1363 (1991); A.W. S. Williams, E. C. Lightowlers, and A. T. Collins, J. Phys. C **3**, 1727 (1970).
[17] C. Persson, A. Ferreira da Silva, and B. Johansson, Phys. Rev. B **63**, 205119, (2001); A. Ferreira da Silva and C. Persson, J. Appl. Phys. **92**, 2550 (2002).
[18] E. Gheeraert, S. Koizumi, T. Teraji, H. Kanda, and M. Nesladek, Phys. Status Solidi A **174**, 39 (1999).
[19] T. H. Borst and O. Weis, Diam. Relat. Mater. **4**, 848 (1995); J.-P. Lagrange, A. Deneuville, and E. Gheeraert,Diam. Relat. Mater. **7**, 1390 (1998).
[20] K. Nishimura, K. Das, and J. T. Glass, J. Appl. Phys. **69**, 3142 (1991); T. Tschepe, J. F. Prins, and M. J. R. Hoch, Diam. Relat. Mater. **8**, 1508 (1999).
[21] M. S. Osofsky, R. J. Soulen Jr. , J. H. Claassen, G. Trotter, H. Kim, and J. S. Horwitz, Phys. Rev. Lett. **87**, 197004 (2001); R. J. Soulen, Jr. and M. S. Osofsky, Phys. Rev. B **68**, 094505 (2003).